# Synthesis of accelerograms compatible with the Chinese GB 50011-2001 design spectrum via harmonic wavelets: artificial and historic records

P.D. Spanos[1*], A. Giaralis[2] and Li Jie[3]

[1] *Professor, L. B. Ryon Chair in Engineering, Rice University, Houston, TX, 77005-1827, USA*

[2] *Post-Doctoral Fellow, Department of Civil and Environmental Engineering, Rice University, Houston, TX, 77005-1827, USA*

[3] *Professor, Institute of Architectural Engineering, Tongji University, Shanghai 200092, China*

**Abstract:** A versatile approach is employed to generate artificial, and to modify field recorded accelerograms which satisfy the compatibility criteria prescribed by the Chinese aseismic code provisions GB 50011-2001. In particular, a frequency dependent peak factor derived by means of appropriate Monte Carlo analyses is incorporated to relate the GB 50011-2001 design spectrum to a parametrically defined evolutionary power spectrum (EPS). Special attention is focused on the definition of the frequency content of the EPS to accommodate the mathematical peculiarities of the aforementioned design spectrum. Further, a one-to-one relationship is established between the parameter controlling the time-varying intensity of the EPS and the effective strong ground motion duration. Subsequently, an efficient auto-regressive moving-average (ARMA) filtering technique is utilized to generate ensembles of non-stationary artificial accelerograms whose average response spectrum is in a close agreement with the considered design spectrum. Furthermore, a harmonic wavelet based iterative scheme is incorporated to modify these artificial signals and field recorded accelerograms pertaining to the May, 2008 Wenchuan seismic event to achieve a close matching of the signals' response spectra with the GB 50011-2001 design spectrum on an individual basis. Zero-phase high-pass filtering is performed to accomplish proper baseline correction of the acquired spectrum compatible artificial and field accelerograms.

---

**Correspodence to:** Pol D. Spanos, George R. Brown School of Engineering, L. B. Ryon Chair in Engineering, Rice University, MS 321, P.O. Box 1892, Houston, TX 77251-1892, U.S.A. E-mail: spanos@rice.edu; Tel: (001)- 713.348.4909

**Keywords:** design spectrum; Chinese aseismic code; artificial accelerograms; evolutionary power spectrum; peak factor; recorded accelerograms; wavelets

## 1 Introduction

The concept of the elastic response spectrum has proven an indispensable tool in describing the hazard posed by seismic events on structured facilities over several years (Chopra, 2007). In this regard, the induced seismic loads are typically represented by means of smooth analytically defined elastic design (response) spectra in the contemporary code provisions for aseismic design of structures (e.g. GB 50011-2001, 2001; Bommer and Ruggeri, 2002; CEN, 2004; ICC, 2006). Furthermore, regulatory agencies allow a certain level of structural damage to occur depending on the severity of the considered seismic action within a performance based design framework. To this aim, inelastic design spectra of reduced spectral ordinates are utilized to account for the expected inelastic/hysteretic response of ordinary structures conforming to certain "regularity" criteria in terms of mass and stiffness distribution in plan and elevation. In this manner, these structures can be conveniently designed by means of linear response spectrum based equivalent static or dynamic analyses incorporating proper modal combination rules. These analyses yield the maximum values of the various quantities of interest to the design process.

Note, however, that explicit consideration of the time-evolving attributes of the structural response becomes critical in addressing the needs of specific earthquake-resistance design scenarios of particular structures. Examples of such structures include important to the community infrastructure that must remain operational after a major seismic event; "irregular" structures; facilities equipped with various passive and/or active vibration control devices for the mitigation of the seismic hazard (e.g. base isolators, energy dissipation devices, tuned-mass dampers, etc); structures housing sensitive secondary/non-structural components; and earth slopes and other

geotechnical engineering constructions. In these cases, aseismic code provisions require dynamic time-history analyses to be performed. In the context of these analyses, the input seismic action is represented by ground acceleration time-histories which should generally reflect the characteristics of the expected strong ground motion in terms of amplitude, frequency content, and duration. To this end, most code regulations world-wide, require a minimum number of time-histories to be considered as input for time-history analysis whose average response spectrum is compatible (i.e. in a close agreement) with a prescribed elastic design spectrum (e.g. Bommer and Ruggeri, 2002). These time-histories can be "real" recorded accelerograms pertaining to historical seismic events, or artificial numerically generated signals derived from an appropriate strong ground motion model.

A plethora of methods can be found in the literature to address the issue of providing response/design spectrum compatible collections of acceleration time-histories for time-history analyses. A relatively recent class of methods involves selecting accelerograms from well-populated data banks and scaling by a constant scalar (e.g. Naeim et al., 2004; Kottke and Rathje, 2008). However, in many instances only a small number of real accelerograms is available to the designer, hopefully recorded at sites corresponding to similar soil conditions and seismogenetic environments with those characterizing the site of the structure to be designed. A common approach to achieve compatibility between the average response spectrum of these accelerograms with a given design spectrum is to modify them deterministically in the time (e.g. Hancock et al., 2006) or in the frequency domain (e.g. Karabalis et al., 2000; Mukherjee and Gupta, 2002; Suarez and Montejo, 2005; Suarez and Montejo, 2007; Das and Gupta, 2008). A different approach involves casting the problem at hand on a probabilistic basis by interpreting the accelerograms as realizations of a "mother" stochastic process characterized in the frequency domain by its power spectrum. In this regard, various researchers have considered the derivation of response/design spectrum consistent stationary power spectra (Gupta and Joshi, 1993; Shrikhade and Gupta, 1996; Falsone and Neri, 2000; Crespi et al., 2002), and evolutionary power spectra (Spanos and Vargas Loli, 1985; Giaralis

and Spanos, 2009) for deriving artificial response spectrum compatible signals via random field simulation (see also Spanos and Zeldin, 1998). In a similar context, a vast amount of literature has been devoted to developing "seismological" models amenable to a frequency domain representation aiming to capture the influence of the seismic fault rupture (source), the seismic waves propagation (path), and the local soil conditions (site) in the strong ground motion (Lam et al., 2000; Ólaffson et al., 2001; Boore, 2003). Eventually, random field simulation techniques are utilized to obtain acceleration time-histories compatible with these models, commonly referred to as "synthetic" accelerograms (e.g. Lam et al., 2000; Bommer and Ruggeri, 2002). Apart from the above standard probabilistic approaches for obtaining artificial/synthetic accelerograms to be used in time-history analysis applications, Iyama and Kuwamura (1999) employed the wavelet transform, Lin and Ghaboussi (2001) considered properly trained stochastic neural networks, Wang et al. (2002) utilized the adaptive chirplet transform and Wen and Gu (2004) incorporated the empirical mode decomposition in conjunction with the Hilbert transform to capture the time-varying frequency content of recorded earthquakes and to simulate non-stationary strong ground motion signals. Furthermore, comprehensive lists of earlier research efforts on the topic at hand can be found in the review articles of Spanos (1983), Preumont (1984), and Carballo and Cornell (2000).

This paper focuses on providing design spectrum compatible accelerograms satisfying the aseismic code provision requirements posed in China by the code GB 50011-2001. For this task, the integrated methodology developed in Giaralis and Spanos (2009) is followed since it encompasses the requisite tools to both generate artificial and manipulate real recorded accelerograms as mandated by the GB 50011-2001 code.

Specifically, the adopted methodology combines two distinct formulations which are further extended and tailored herein to accommodate the GB 50011-2001 code. The first formulation involves the approximate solution of an inverse stochastic dynamics problem to relate a parametrically defined evolutionary power spectrum (EPS) to a given design spectrum via the

concept of the "peak factor" (see also Vanmarcke, 1976; Spanos and Vargas Loli, 1985). In this respect, artificial accelerograms can be generated as samples of the design spectrum-consistent EPS. An efficient state-of-the-art filtering technique relying on an auto-regressive moving-average (ARMA) discrete-time filter is utilized for this purpose. Special attention is given to establish a relationship between the effective strong ground motion duration and the relevant parameter controlling the time-evolving property of the parametric EPS form. The frequency content of the latter is defined via the well-known Kanai-Tajimi spectrum (Kanai, 1957), which obviously should be construed as a purely mathematical instrument. Furthermore, a GB 50011-2001 design spectrum consistent frequency dependent peak factor is derived via pertinent Monte Carlo simulations.

The second formulation of the adopted methodology utilizes the family of harmonic wavelets (Newland, 1994) for modifying iteratively individual accelerograms to achieve a close agreement of their response spectra with a target design spectrum (see also Mukherjee and Gupta, 2002). This iterative procedure is applied to the artificial signals simulated based on the first formulation to improve the agreement of their response spectra with the GB 50011-2001 design spectrum on an individual basis. Furthermore, treatment of real recorded accelerograms by the aforementioned wavelet-based iterative procedure is also adopted for meeting the compatibility criteria of the GB 50011-2001 code provisions. In particular, a detailed design example is included in which certain accelerograms recorded during the May, 2008 Wenchuan event are iteratively modified to achieve enhanced matching of the associated response spectral ordinates with a target spectrum defined in conjunction with GB 50011-2001.

In all of the aforementioned tasks, appropriate base-line correction is achieved by ad-hoc acausal zero-phase high-pass filtering.

## 2 Simulation of artificial spectrum compatible earthquake records

### 2.1 Adopted parametric non-stationary model for strong ground motion

Consider a sample of a zero-mean separable non-stationary stochastic process represented in the domain of time $t$ as the product of a deterministic time-dependent envelop function $A(t)$ with a zero-mean stationary stochastic process $y(t)$; it is meant to model the ground acceleration $u_g(t)$ due to a seismic event, that is,

$$u_g(t) = A(t)\, y(t). \tag{1}$$

Assuming that $A(t)$ varies slowly with time, the non-stationary process $u_g(t)$ can be characterized by a two-sided evolutionary power spectrum (EPS) $G(t,\omega)$ in the domain of frequency $\omega$ given by the equation (Priestley, 1965)

$$G(t,\omega) = |A(t)|^2\, Y(\omega) \quad , \quad |\omega| \le \omega_b ; \tag{2}$$

in this equation $Y(\omega)$ denotes the band-limited stationary power spectrum of the stationary stochastic process $y(t)$, and $\omega_b$ is the highest frequency of interest. The above model has been used extensively in the literature to capture the evolutionary attributes of the intensity exhibited by typical recorded seismic accelerograms pertaining to historic seismic events. That is, an initial period of development followed by a relatively slow decay in time. Various parametric forms of envelop functions have been proposed in the literature for the purpose; a comprehensive list can be found in Jangid (2004). Herein, the exponential modulated function given by the expression (Bogdanoff et al., (1961))

$$A(t) = Ct \exp\left(-\frac{b}{2}t\right) , \tag{3}$$

is adopted. In Eq. (3), $C$ is a parameter proportional to the intensity of the ground acceleration process while the $b$ parameter controls the shape of the envelop function. Specifically, it is easy to verify that the maximum value attained by the function $A(t)$ occurs at $t_{max}= 2/b$ and is equal to

$A_{\max} = \dfrac{2C}{b\exp(1)}$ . Furthermore, by considering the time-dependent cumulative energy *E(t)* of the process $u_g(t)$ given by the equation

$$E(t) = \int_0^t \int_{-\omega_b}^{\omega_b} G(\tau,\omega)\, d\omega d\tau \,, \tag{4}$$

and by adopting the effective strong-ground motion duration as defined by Trifunac and Brady (1975), that is,

$$T_{eff} = t_{95} - t_{05} \,, \tag{5}$$

where

$$E(t_{95}) = 0.95E(t\to\infty) \quad ; \quad E(t_{05}) = 0.05E(t\to\infty), \tag{6}$$

the following relations are derived by using Eqs. (2)~(4) and (6) (see also Quek et al., 1990):

$$\left(b^2t_{95}^2 + 2bt_{95} + 2\right)\exp\left(-bt_{95}\right) = 0.1 \quad ; \quad \left(b^2t_{05}^2 + 2bt_{05} + 2\right)\exp\left(-bt_{05}\right) = 1.9\,. \tag{7}$$

Clearly, Eqs. (5) and (7) establish a non-linear relationship between the effective duration and the parameter *b*. A plot of this relationship is given in Fig. 1, while Fig. 2 includes plots of the envelop function of Eq. (3) normalized by $A_{max}$, and of the corresponding cumulative energy *E(t)* normalized by the total energy $E(t\to\infty)$ for various values of *b*. It is noted that similar results can be readily derived by considering any other of the numerous definitions of the effective duration of strong ground motion found in the literature (see e.g. Bommer and Martínez-Pereira, 1999 and references therein). It is further pointed out that selecting large values for the *b* parameter may violate the "slowly-varying" attribute of the envelop function which must hold for Eq. (2) to be valid. In a recent work, Politis et al. (2006) verified that Eq. (2) holds within engineering precision for $b$= 0.5 ($T_{eff}$= 11s) by employing the adaptive chirplet transform.

In accounting for the frequency content of the ground acceleration process, any of the various phenomenological (see e.g. Lutes and Lilhanand, 1979; Clough and Penzien, 1993; Falsone and Neri, 2000; Giaralis and Spanos, 2009) or seismological models (see e.g. Lam et al., 2000;

Ólaffson et al., 2001; Boore, 2003) can be used to represent the power spectrum function $Y(\omega)$ in Eq. (2). In this work, the Kanai-Tajimi (K-T) power spectrum (Kanai, 1957) is adopted which has been widely used in strong ground motion characterization (e.g. Lai, 1982), and in simulation of earthquake accelerograms (e.g. Conte et al., 1992). Mathematically, it relates to the squared absolute value of the frequency response function of a single-degree-of-freedom (SDOF) system with ratio of critical damping $\zeta_g$ and natural frequency $\omega_g$. That is,

$$Y(\omega) = \frac{1 + 4\zeta_g^2 \left(\omega / \omega_g\right)^2}{\left(1 - \left(\omega / \omega_g\right)^2\right)^2 + 4\zeta_g^2 \left(\omega / \omega_g\right)^2} \quad , \quad |\omega| \le \omega_b \,, \tag{8}$$

in which $\zeta_g$ and $\omega_g$ account for the filtering effects of the surface soil deposits. The choice of the K-T spectrum has been dictated by the attributes of the analytical expression adopted in the current Chinese aseismic code provisions (GB 50011-2001) for the definition of the design spectrum (see the Appendix A). In particular, the last segment of the pseudo-acceleration response spectrum pertaining to the range of long natural periods yields monotonically increasing relative displacement spectral ordinates. This trend excludes the incorporation of a high-pass filter in modeling the frequency content of the $u_g$ process which is usually included to suppress low frequency components allowed by the K-T spectrum (see e.g. Clough and Penzien, 1993; Giaralis and Spanos, 2009).

### 2.2 Formulation and approximate solution of an inverse stochastic dynamics problem

Consider a linear quiescent unit-mass SDOF oscillator with $\zeta_n$ ratio of critical damping and $\omega_n$ natural frequency base-excited by the acceleration process $u_g(t)$. The motion of this system is governed by the equation

$$\ddot{x}(t) + 2\zeta_n \omega_n \dot{x}(t) + \omega_n^2 x(t) = -u_g(t) \quad ; \quad x(0) = \dot{x}(0) = 0 \,, \tag{9}$$

where $x(t)$ is the relative displacement process of the oscillator with respect to the motion of its base, and a dot over a quantity denotes differentiation with respect to time. Given a relative displacement

design/response (target) spectrum $S_d$, it is possible to relate it with an EPS $G(t,\omega)$ using the equation (Spanos and Vargas Loli, 1985)

$$S_d\left(\omega_n,\zeta_n\right)=r\left(\omega_n,\zeta_n,G\right)\max_t\left\{\sigma\left(t,\omega_n,\zeta_n,G\right)\right\}. \tag{10}$$

In the above equation, $\sigma$ is the time-evolving variance of the amplitude of the relative displacement response process $x$. It has been proved by Spanos and Lutes (1980) that for lightly damped oscillators ($\zeta_n<<1$) excited by relatively broad-band input excitations a reliable expression for the variance $\sigma$ is provided by the equation

$$\sigma^2\left(t\right)=\frac{\pi}{\omega_n^2}\exp\left(-2\zeta_n\omega_n t\right)\int_0^t\exp\left(2\zeta_n\omega_n\tau\right)G\left(\tau,\omega_n\right)d\tau\,. \tag{11}$$

Furthermore, the symbol $r$ in Eq. (10) denotes the so-called "peak factor": the critical parameter establishing the equivalence, within a certain probability/ confidence level, between the target $S_d$ and the EPS $G(t,\omega)$ (see e.g. Vanmarcke, 1976). In general, the peak factor depends on the dynamic properties of the SDOF oscillator considered ($\omega_n$, $\zeta_n$), and on the frequency content and duration of the input process, but not on the energy/intensity of the excitation. It is closely related to the first-passage problem in the field of random vibrations for which no exact convenient solution is known. Several researchers have provided approximate expressions to estimate $r$ for non-stationary input processes (see e.g. Mason and Iwan, 1983; Michaelov et al., 2001; Morikawa and Zerva, 2008) obtained under various restrictive conditions to solve the forward problem defined by Eq. (10), namely to obtain the response spectrum $S_d$ for a given input EPS. However, most of these expressions tend to be rather involved mathematically and depend on the SDOF system response statistics, a fact which significantly hinders the solution of the inverse problem of Eq. (10) (i.e. given an $S_d$ derive a compatible EPS). To circumvent these difficulties, previous related studies have assumed a constant value for $r$ appropriately selected to provide conservative results, that is, processes yielding realizations whose average response spectra would lie above the target design spectrum (Spanos and Vargas Loli, 1985; Marano et al., 2008; Giaralis and Spanos, 2009). In this

paper, natural frequency dependent peak factors are derived by means of appropriate Monte Carlo simulations and used in conjunction with Eq. (10) to achieve a closer matching of the response spectra of samples characterized by the obtained EPS on the average. Further details on this issue and numerical results are provided in section 5.

A point-wise approximate solution to the inverse problem of Eq. (10) can be obtained, as has been originally suggested by Spanos and Vargas Loli (1985), which seeks to satisfy Eq. (10) at a certain set of frequencies $\{\omega_{n(j)}\}$ for $j$= 1,…,$M$, in the least square sense. To this aim, a standard over-determined non-linear least-square fit optimization problem is formulated as follows (see also Giaralis and Spanos, 2009)

$$\min\left\{\sum_{j=1}^{2M}\left(S_j-\sigma_j\right)^2\right\}, \tag{12}$$

where

$$S_j=\begin{cases} S_d^2\left(\omega_{n(j)},\zeta_n\right) & , \quad j=1,...,M \\ 0 & , \quad j=M+1,...,2M \end{cases}, \tag{13}$$

and

$$\sigma_j=\begin{cases} \dfrac{r^2\pi C^2 t_j^{*2}\exp\left(-bt_j^*\right)}{2\zeta\omega_{n(j)}^3}Y\left(\omega_{n(j)}\right) & , \quad j=1,...,M \\ \gamma_{j-M}^2\left(2t_{j-M}^*-bt_{j-M}^{*2}\right)-2\gamma_{j-M}\left(1-bt_{j-M}^*\right)- & \\ -2b+4\zeta_n\omega_{n(j-M)}\exp\left(-\gamma_{j-M}t_{j-M}^*\right) & , \quad j=M+1,...,2M \end{cases}, \tag{14}$$

where

$$\gamma_j=2\zeta_n\omega_{n(j)}-b\,. \tag{15}$$

In Eqs. (12)-(15) the unknowns to be determined are the set of $M$ time instants $\{t_j^*\}$ at which the variance $\sigma$ corresponding to the oscillator with natural frequency $\omega_{n(j)}$ is maximized, the intensity parameter $C$, the envelop shape parameter $b$ and the K-T parameters $\omega_g$ and $\zeta_g$, while the total number of equations is $2M$. In all of the ensuing numerical results, a standard Levenberg-Marquardt

algorithm with line search is utilized (see e.g. Nocedal and Wright, 1999) to solve the optimization problem defined by Eqs. (12)-(15) at several tenths of points $\{\omega_{n(j)}\}$ along the frequency band of interest as detailed in section 5.

### 2.4 On the simulation of artificial earthquake accelerograms using ARMA models

Obviously, by solving Eqs. (12)-(15) for a given target design spectrum complete determination of the parametrically defined EPS $G(t,\omega)$ is achieved. Next, any appropriate random field generation method can be utilized to synthesize an arbitrarily large number of non-stationary accelerograms as realizations of the underlying stochastic process $u_g$ characterized by the obtained EPS. Employing a uniformly modulated (separable) EPS allows this task to be performed in a two-step procedure. In this regard, at first, discrete stationary time-histories compatible with the K-T spectrum $Y(\omega)$ of Eq. (8) are generated. These records can be interpreted as sampled versions of realizations of the band-limited continuous-time process $y$

$$y[k] = y(kT_s) \quad , \quad k \in \mathbb{Z}, \tag{16}$$

where the sampling interval $T_s$ must obey the Nyquist criterion to avoid aliasing. Namely,

$$T_s \leq \frac{\pi}{\omega_b}. \tag{17}$$

Next, these stationary records are multiplied individually by the corresponding discrete/sampled version of the envelop function defined in Eq. (3) to obtain the final artificial records with non-stationary intensity as Eq. (1) suggests.

Several methods for generating discrete-time stationary signals compatible with a prescribed power spectrum are available in the literature. Spanos and Zeldin (1998) have reviewed the most common of the methods and commented on their main attributes and relative advantages. Herein, a filtering method incorporating an autoregressive-moving-average (ARMA) model is used for the purpose: a common choice for modeling and simulating strong ground motions (see e.g. Kozin

(1988); Conte et al., (1992); Ólaffson et al., 2001). The objective of this simulation method is to "color" a discrete-time Gaussian white noise process $w$ band-limited to $\omega_b$ possessing the autocorrelation function $R_{ww}$ and the power spectrum $W(\omega)$

$$R_{ww} = E\{w[u]w[v]\} = \begin{cases} 2\omega_b\,, u = v \\ 0\,, u \neq v \end{cases} \quad ; \quad W(\omega) = 1\,, |\omega| \leq \omega_b \ , \tag{18}$$

in which E{•} is the operator of mathematical expectation by passing it through an ARMA($p$,$q$) filter. The latter filter has a frequency response function $H$ given by the equation

$$H\left(e^{i\omega T_s}\right) = \frac{\sum_{l=0}^{q} c_l e^{-li\omega T_s}}{1 + \sum_{s=1}^{p} d_s e^{-si\omega T_s}} \quad ; \quad i = \sqrt{-1}\,. \tag{19}$$

where $c_l$ ($l$=0,1,…,$q$) and $d_s$ ($s$=0,1,…,$p$) are appropriate coefficients with $d_0$=1.

In the discrete-time domain the aforementioned filtering operation is governed by the difference equation

$$\tilde{y}[k] = -\sum_{s=1}^{p} d_k \tilde{y}[k-s] + \sum_{l=0}^{q} c_l w[k-l], \tag{20}$$

from which it can be readily understood that the $k$-sample of the output process $\tilde{y}$ of the ARMA($p$,$q$) model is calculated recursively as a linear combination of the previous $p$ samples plus a convolution term involving the white input noise.

There are several methods available for determining appropriate ARMA filter coefficients to match the power spectrum $\left|H\left(e^{i\omega T_s}\right)\right|^2$ of the process $\tilde{y}$ with the K-T spectrum $Y(\omega)$. Clearly, if this is successfully accomplished, then the process $\tilde{y}$ defined in Eq. (20) can reliably replace/model the target discrete process $y$ of Eq. (16). Herein, the auto/cross-correlation matching (ACM) method is utilized (see Spanos and Zeldin, 1998). According to this method, a relatively long pure autoregressive (AR) filter is defined to model $y$ at an initial stage. Then, the output auto-correlation and the input/output cross-correlation arrays between this preliminary AR and the final ARMA

model are equated. Finally, the coefficients of the desired ARMA($p$,$q$) filter are determined by solving a $p$+$q$ by $p$+$q$ system of linear equations, where the values of $p$ and $q$ can be chosen at will to achieve any level of matching between the target spectrum $Y(\omega)$ and the squared modulus of the frequency response function of the ARMA($p$,$q$) filter. The mathematical details of the adopted ACM method are included in Spanos and Zeldin, (1988).

**3 Deterministic iterative response spectrum matching procedure using harmonic wavelets**

As it has already mentioned in the introductory section of this paper, a plethora of methods exists to modify both historic and artificially generated accelerograms deterministically to achieve enhanced agreement between their response spectra with a target design spectrum. In the case of recorded accelerograms pertaining to historic seismic events this need stems from the fact that their response spectra are usually rather irregular and "jagged" compared to the smooth design spectra corresponding to the same level of intensity/ peak ground acceleration. Moreover, the response spectra of individual artificial accelerograms generated from procedures as the one described in the preceding section are not guaranteed to achieve a sufficient level of matching with a given design spectrum (see also Spanos and Vargas Loli, 1985; Giaralis and Spanos, 2009). To this aim, the use of harmonic wavelets in conjunction with an iterative numerical procedure proposed by Giaralis and Spanos (2009) is employed in the ensuing numerical examples to treat both artificially generated and accelerograms recorded during the Wenchuan earthquake (May, 2008) to enhance the agreement of their response spectra with the design spectrum prescribed by the Chinese aseismic code provisions GB 50011-2001 (Appendix A).

Specifically, a harmonic wavelet of ($m$,$n$) scale and $k$ position in time $\psi_{(m,n),k}(t)$ is defined in the frequency domain by the equation (Newland, 1994)

$$\Psi_{m,n}(\omega)=\begin{cases}\dfrac{1}{(n-m)\Delta\omega}\exp\left(\dfrac{-i\omega kT_o}{(n-m)}\right) & , \quad m\Delta\omega\le\omega\le n\Delta\omega \\ 0 & , \quad otherwise\end{cases}, \tag{21}$$

which corresponds to an ideal band-pass filter. In Eq. (21) $m$, $n$, and $k$ are assumed to be positive integer numbers, and

$$\Delta\omega=\frac{2\pi}{T_o}, \tag{22}$$

where $T_o$ denotes the total length of the time interval considered in seconds. Note that, Newland (1994) showed via energy preservation arguments that a collection of harmonic wavelets spanning adjacent non-overlapping bands at different ($m$,$n$) scales along the frequency axis constitutes a complete and orthogonal basis for finite energy functions. Hence, the harmonic wavelet transform (HWT) expressed in the time domain by the formula

$$\left[W_\psi f\right](m,n,k)=\frac{n-m}{T_o}\int_0^{T_o} f(t)\overline{\psi_{(m,n),k}(t)}dt, \tag{23}$$

in which the bar over a symbol denotes complex conjugation, can be utilized to decompose any real-valued finite energy signal $f(t)$ into sub-signals $f_{m,n}(t)$, so that, (Spanos et al., 2005; Spanos et al., 2007)

$$f(t)=\sum_{m,n} f_{m,n}(t), \tag{24}$$

where

$$f_{m,n}(t)=2\,\mathrm{Re}\left\{\sum_{k=0}^{n-m-1}\left[W_\psi f\right](m,n,k)\psi_{(m,n),k}(t)\right\}. \tag{25}$$

In this respect, the response of a lightly damped SDOF oscillator of natural frequency within an interval $[m_j\Delta\omega,n_j\Delta\omega]$ excited by an accelerogram $f(t)$ would be mainly influenced by the $f_{mj,nj}(t)$ part of the $f(t)$ signal. Thus, an iterative modification procedure can be devised to scale all sub-signals at the $v$-th iteration according to the equation (Mukherjee and Gupta, 2002)

$$f_{m,n}^{(v+1)}(t) = f_{m,n}^{(v)}(t) \frac{\int_{m\Delta\omega}^{n\Delta\omega} S_d(\omega)\, d\omega}{\int_{m\Delta\omega}^{n\Delta\omega} D^{(v)}(\omega)\, d\omega} \tag{26}$$

to improve the agreement of the response spectrum of an accelerogram $f(t)$ with a target spectrum $S_d$. In Eq. (26), $D^{(v)}(T)$ denotes the displacement response spectrum related to $f^{(v)}(t)$ obtained by Eq. (24) at each iteration.

From a numerical implementation perspective, the fast Fourier transform based algorithms presented in Newland (1998) can be employed for the efficient computation of the convolution integral of Eq. (23) in the frequency domain. Moreover, a sufficient number of [$m\Delta\omega$, $n\Delta\omega$] "bins" need to be considered to cover all frequencies of interest. A related detailed discussion along with numerical evidence on the impact of the length of these bins on the efficiency of the above described iterative procedure can be found in Giaralis and Spanos (2009). In general, it is noted that harmonic wavelets offer certain computational advantages over the wavelet families considered by Mukherjee and Gupta (2002) and Suarez and Montejo (2005), in the context of similar iterative procedures advocated in these references, especially when enhanced agreement is mandated only at a certain band of frequencies (Giaralis and Spanos, 2009). Notably, this is the case of the compatibility criteria prescribed by aseismic code provisions currently effective in Europe (CEN, 2004) and in the United States (ICC, 2006).

## 4 Acausal high-pass filtering for baseline adjustment

It can be readily seen form Eq. (8) that the K-T spectrum does not vanish as $\omega \rightarrow 0$ and thus allows low-frequency components in the acceleration time-histories which results in abnormalities in the displacement traces and in the corresponding relative displacement response spectra (e.g. Clough and Penzien, 1993; Giaralis and Spanos, 2009). Thus, it is necessary to treat the non-stationary artificially generated K-T spectrum compatible signals by a high-pass filter with a

relatively low cut-off frequency to suppress these low frequency components (see also Chopra and Lopez, 1979; Conte et al., 1992; Karabalis et al, 2000). In essence, this can be interpreted as a base-line correction operation which also constitutes an important step in processing raw recorded seismic signals (Boore and Bommer, 2005). Furthermore, similar baseline correction considerations are necessitated in dealing with the accelerograms scaled/modified by the iterative procedure described in the previous section (Montejo and Suarez, 2007; Giaralis and Spanos, 2009). To this aim, high-pass acausal filtering incorporating a fourth order Butterworth filter with cut-off frequency of 0.10Hz is performed to address the needs for baseline adjustments in both the artificially generated and real recorded accelerograms considered in the following section (Converse and Brady, 1992). Specifically, zero-padding of sufficient length is first introduced before the start and at the end of each accelerogram to provide sufficient time length for the expected end-effects of the acausal filtering to be rectified (Boore, 2005). Next, the thus padded accelerograms are filtered in the forward direction using the aforementioned filter. The filtered signals are then reversed in time and pass through the same filter for a second time. In this manner, zero-phase filtering is accomplished which minimizes the impact of the properties of the filter considered on the shape of the displacement time-histories and the long period response spectral ordinates (Chopra and Lopez, 1979; Boore and Akkar, 2003). The latter is an important advantage of the adopted baseline correction technique since it practically has insignificant effect on the quality of spectral matching achieved via the wavelet-based modification procedure (Giaralis and Spanos, 2009).

## 5 Application to the design spectrum of the current Chinese aseismic code: GB 50011-2001

### 5.1 Derivation of non-constant peak factors via Monte Carlo simulations

In formulating the stochastic simulation problem of section 2.2 a response spectrum has been related to a non-stationary stochastic process via Eq. (10) by considering the concept of the peak factor $r$. For the purposes of this study, $r$ is construed as the ratio of the average peak response $x$

over the maximum response variance of a SDOF system subject to a non-stationary random process $u_g$ characterized by the EPS $G$ in the frequency domain (see also Eq. (9)). In this regard, Eq. (10) establishes the following compatibility criterion between a design/response spectrum $S_d$ and an EPS $G$: considering an ensemble of non-stationary samples compatible with $G$ (i.e. generated as described in section 2.4), half of the population of their response spectra will lie below $S_d$ (i.e. $S_d$ is the median response spectrum).

Relying on this interpretation of the peak factor, it is possible to estimate $r$ corresponding to a SDOF with ratio of critical damping $\zeta_n$ and natural period $T_n = 2\pi/\omega_n$ excited by a specific EPS $G$ numerically by relying on the equation

$$r\left(T_n,\zeta_n,G\right)=\frac{E\left\{\max_t\left\{\left|x\left(t,T_n,\zeta_n,G\right)\right|\right\}\right\}}{\max_t\left\{\sqrt{E\left\{x^2\left(t,T_n,\zeta_n,G\right)\right\}}\right\}}. \tag{27}$$

For a fixed damping ratio $\zeta_n$ and input EPS the above equation yields the so-called average (median) peak factor spectrum ($r$-spectrum) (Vanmarcke, 1976).

To this end, a Monte Carlo analysis is undertaken to derive natural period dependent peak factors pertaining to the Chinese aseismic code provisions (GB 50011-2001), for $\zeta_n = 0.05$. In particular, evolutionary K-T spectra are obtained for all 14 possible values of the characteristic period $T_g$ (see the Appendix A), by solving the optimization problem defined by Eqs. (12)~(15) . Specifically, a point-wise matching is pursued at 70 frequencies $\omega_{n(j)}$ judicially distributed onto the interval $[\max\{2\pi/(6.5T_g),\ 2\pi/(6)\},\ 314.16]$ (rad/s) which is mapped onto the interval $[0.02,\ \min\{6.5T_g,\ 6\}]$ (s) on the axis of natural periods (see also Giaralis and Spanos, 2009). For these analyses $\alpha_{max}$ is set equal to 0.50g, and a constant peak factor $r = (3\pi/4)^{1/2}$ is assumed. For each of the thus derived spectra a suite of 10000 spectrum-compatible non-stationary artificial accelerograms is generated and base-line adjusted as described in sections 2.4 and 4. Next, the responses of a series of 200 SDOF oscillators with natural periods ranging from $T = 0.02$s to $T = 6$s and with $\zeta_n = 0.05$

damping ratio excited by the above suites of accelerograms are calculated through Eq. (9). Figure 3 shows all individual *r*-spectra pertaining to the thus obtained responses computed via Eq. (28) (thin black lines). Clearly, each such spectrum is associated with a GB 50011-2001 design spectrum of a specific shape controlled by the $T_g$ parameter. Evidently, the peak factor has a complex dependency with the natural period of linear SDOF oscillators. Interestingly, similar trends for *r*-spectra derived from stationary K-T input processes have been previously reported in the literature (Vanmarcke, 1976). In passing, it is pointed out that the ratio defined in Eq. (28) is independent of the intensity of the input process considered. Hence, the derived *r*-spectra of Fig. 3 are not influenced by the constant value of the peak factor and the value of $\alpha_{max}$ adopted to obtain the GB 50011-2001 design spectrum compatible K-T spectra considered in the aforementioned Monte Carlo simulations.

Arguably, the most important conclusion deduced from Fig. 3 is that the *r*-spectra are relatively insensitive to the shape of the GB 50011-2001 design spectrum since they are closely clustered for all natural period considered. In this regard, it is reasonable to fit a polynomial in the least square sense to the average of the numerically derived *r*-spectra curves. In this manner, an analytic expression for a GB 50011-2001 design spectrum compatible peak factor spectrum is reached which does not dependent on the $T_g$ parameter. Specifically, the eighth-order polynomial superimposed in Fig. 3 (thick gray curve) and expressed by the equation

$$r\left(T,\zeta_n=0.05\right)=\sum_{j=0}^{8}p_jT^j\ ,\ 0.02s\le T\le 6\mathrm{s} \tag{28}$$

is found to approximate satisfactorily the average peak factor spectrum. The polynomial coefficients $p_j$ are reported in Table 1. Clearly, the peak factor spectrum of Eq. (28) can be incorporated in Eq. (14) to obtain EPSs compatible with the various shapes of the GB 50011-2001 design spectrum as described in the following section.

**5.2 Design spectrum compatible evolutionary K-T spectra and artificial accelerograms**

Table 2 shows the requisite parameters for the determination of evolutionary K-T spectra compatible with the GB 50011-2001 design spectrum for all possible combinations of the quantities $T_g$ and $\alpha_{max}$ (Appendix A). Both design levels corresponding to the "frequent" earthquake event (return period of 50 years) and to the "rare" earthquake event (return period of 2000 years) are considered. These spectra have been derived by solving the minimization problem of Eqs. (12)~(15) and incorporating in Eq. (14) the natural period dependent peak factor of Eq. (29). Figure 4 provides examples of the quality of the point-wise matching on the interval $[0.02, \min\{6.5T_g, 6\}]$ (s) achieved for various values of $T_g$ and $\alpha_{max}$ in terms of the relative displacement and pseudo-acceleration spectral ordinates. Furthermore, Fig. 5 shows the average and median response spectra of ensembles of non-stationary seismic accelerograms compatible with the same K-T spectra considered in Fig. 4. Each ensemble includes 40 signals generated by means of the ARMA method discussed in section 2.4 and baseline adjusted via high-pass filtering as described in section 4.

Examining the results presented in Fig. 4, it is clear that the adopted parametric model (evolutionary K-T) does not include enough "degrees of freedom" (i.e. number of free parameters) to allow the optimization algorithm to trace the GB 50011-2001 design spectrum throughout the axis of natural periods with the same effectiveness. Better point-wise matching can be accomplished via models encompassing more degrees of freedom such as the one adopted in Spanos and Vargas Loli (1985) involving the superposition of more than one uniformly modulated K-T spectra (see also Falsone and Neri (2000) and Crespi et al., (2002) who considered a simpler stationary version of the problem at hand). However, these models yield non separable evolutionary processes for the characterization of strong ground motion whose complexity may limit their practical merits. Furthermore, it is noted that improved matching between the target spectrum and the obtained spectral ordinates computed via Eq. (10) for a given EPS $G$ (forward problem), does not necessarily guarantee enhanced agreement between the average response spectra of the generated EPS

compatible accelerograms with the target spectrum, especially for a relatively low number of generated accelerograms. In fact, the achieved agreement of the average response spectra of the generated accelerograms compatible with the simple evolutionary K-T models is certainly acceptable by common engineering criteria in the range of periods shorter than $5T_g$ as evidenced by Fig 5. In general, it is perhaps more practical to pursue an improved agreement via deterministic treatment of the generated signals using, for instance, the continuous wavelet transform as described in the next section, rather than by utilizing more sophisticated parametric expressions for the EPS.

Another issue that deserves further comments is the poor agreement of the average response spectra of the generated base-line corrected accelerograms with the target design spectrum under consideration. This is due to the fact that the K-T spectrum cannot capture the relatively slow linear rate of decay of the last segment of the GB 50011-2001 pseudo-acceleration design spectrum. In fact, it is noted that the optimization algorithm fails to converge to physically meaningful K-T parameters if the interval of point-wise matching is stretched to include periods longer than approximately $6.5T_g$. To this end, it is pointed out that although no reference is made in GB 50011-2001 about the relative displacement design spectrum and its shape, the assumption of linearly decaying pseudo-acceleration spectral ordinates in the range of long periods yields monotonically increasing spectral ordinates in terms of relative displacements as the stiffness of the linear SDOF oscillators decreases. This trend deviates somewhat from what is prescribed in other contemporary aseismic code provisions such as the European EC8 (CEN, 2004) and from what is observed in recorded accelerograms (e.g. Faccioli et al., 2004), and perhaps it deserves additional scrutinizing. Moreover, it does not allow the consideration of more sophisticated phenomenological models such as the Clough-Penzien spectrum (Clough and Penzien, 1993; Giaralis and Spanos, 2009),which provide a more reliable characterization of the strong ground motion in the range of low-frequencies (i.e. longer periods).

Parenthetically, it is noted that the formulation of section 2.2 allows for choosing a shape parameter *b a priori* to achieve a desirable effective duration in the generated artificial accelerograms by solving numerically Eqs. (5) and (7) or by using the graph of Fig. 1. Then, *b* can be treated as a constant, instead of a free parameter, and be left out of the optimization problem of Eqs. (12)~(15). This feature further enhances the versatility of the proposed stochastic method and can significantly facilitate the aseismic design of structures in cases where the effective duration of the input strong ground motion is deemed as an important designing parameter (see e.g. Iervolino et al., 2006; Hancock and Bommer, 2006).

**5.3 Enhanced design spectrum compatible matching via the harmonic wavelet transform**

In this section a specific design scenario is considered to illustrate the usefulness and applicability of the harmonic wavelet based iterative matching procedure of section 3 to satisfy the compatibility criteria of the GB 50011-2001 regulations. Specifically, it is set to design a structure classified at the highest category of importance (i.e. a structure whose failure will have significant secondary consequences), located at the capital of China, Beijing, founded on surface soil layers that fall within the description of soil-type 2 (i.e. relatively stiff soil deposits), for the "rare" earthquake event according to the GB 50011-2001. Furthermore, suppose that a non-linear dynamic time-history analysis is deemed essential to be included in the design process. In this case the current Chinese aseismic code provisions mandate to considering at least two sets of recorded earthquake accelerograms and one set of artificial earthquake records to be used as input for the aforementioned analysis. Each set of signals consists of two horizontal orthogonal components assumed to act along the principal axes of the structure to be designed. The average response spectra of the above signals on each direction must be in conformity (i.e. in a close agreement) with the GB 50011-2001 design (target) spectrum corresponding to $T_g$=0.40s and $\alpha_{max}$= 1.40g (see also Shiping, 1993 and Appendix A).

To accommodate the above requirements, the horizontal orthogonal components (East-West or E-W and North-South or N-S) of seismic accelerograms recorded in two different sites during the May, 2008 Wenchuan earthquake of magnitude 7.9 are considered, hereafter named by Wenchuan 1 and 2. These have been retrieved from raw data by means of standard techniques and base-line adjusted as detailed in section 4 (see also Boore and Bommer, 2005 and the therein references). Additionally, two artificial accelerograms compatible with the evolutionary K-T spectrum taken from Table 2 associated with the prescribed GB 50011-2001 target spectrum (with $T_g$=0.40s and $\alpha_{max}$= 1.40g) are also generated. The two E-W recorded components together with one of the two artificial signals, namely artificial 1, are grouped together assuming that they will act along the same principal axis of the structure to be designed in the context of the requisite inelastic dynamic analysis. Accordingly, a second group of signals comprising the remaining three signals, that is, the two N-S recorded components and the second artificial signal (artificial 2), is formed acting along the second structural principal axis.

Plots of the acceleration and displacement traces of the aforementioned groups of signals are shown in the first and the third "columns" of panels in Fig. 6, respectively. Moreover, Fig. 7 includes the individual response spectra of both groups of signals in terms of pseudo-acceleration and relative displacement. In the same figure the average response spectra of each group are also provided and compared with the target spectrum. Obviously, the level of agreement is relatively poor throughout the axis of natural periods considered. To rectify this shortcoming, the iterative harmonic wavelet based matching procedure of section 3 is used to modify individually the considered signals to improve the agreement of the average response spectra of each group with the GB 50011-2001 target spectrum. Specifically, all signals are projected on a harmonic wavelet basis spanning the frequency domain up to the Nyquist frequency by scales of constant bandwidths with $n$-$m$= 6 and $\Delta\omega$= *0.0767*rad/s via Eq. (23). Then, the obtained sub-signals are iteratively scaled by means of Eq. (26). At each iteration the sub-signals are summed to retrieve the complete modified

accelerogram as suggested by Eq. (24). After eight iterations the discrepancy between the average response spectra of the considered groups of modified accelerograms and the target spectrum gauged by the RMS error (Giaralis and Spanos, 2009)

$$RMS\ error = \sqrt{\frac{1}{N_k}\sum_{j=1}^{N_k}\left(\frac{S_d\left(T_j\right)-D\left(T_j\right)}{S_d\left(T_j\right)}\right)^2} \tag{29}$$

falls well below 6% as shown in Fig. 8. In Eq. (29) $D$ signifies the average relative displacement response spectrum of a group of signals. The RMS error curves of Fig. 8 have been evaluated at $T_j$= 1,…,$N_k$(=300) equally spaced points on the interval [0.02, 6] (s). In Fig. 6 the modified (matched) accelerograms and their associated displacement time-histories obtained after eight iterations as described above are juxtaposed with the "unmodified" (original) time-histories considered. Furthermore, the individual and group averaged pseudo-acceleration and relative displacement response spectra of the thus modified signals are shown in Fig. 9 along with the target spectrum to assess the quality of matching achieved.

The effectiveness of the proposed harmonic wavelet based iterative procedure to modify both "real" recorded and artificially generated signals to meet the compatibility criteria with the design spectrum of the Chinese aseismic regulations GB 50011-2001 is readily seen by comparison of Figs. 7 and 9. Incidentally, it is observed that the requisite modifications induced by the proposed method pertain mostly to the low frequency composition of the treated signals. This can be deduced by the dramatic amplification of the displacement time-histories before and after being processed via the iterative matching procedure, especially in the case of the recorded accelerograms (see Fig. 6). It is noted that from a signal processing viewpoint the displacement time-histories constitute low-pass filtered versions of the corresponding acceleration traces and thus reflect the richness of the earthquake records in low frequencies. This extensive enrichment of the low frequency content in the modified accelerograms is a consequence of pursuing a close matching of their response spectra with the GB 50011-2001 design spectrum for periods longer than $5T_g$ which equals to 2s in the case

considered. However, it is known that such low frequency content is rarely observed in recorded earthquake accelerograms as it can be witnessed by the displacement traces of the original Wenchuan records considered (see also Faccioli et al., 2004 and Boore and Bommer, 2005). Obviously, the monotonically increasing behavior of the GB 50011-2001 relative displacement design spectrum for $T>5T_g$ results in such unusual spectrum compatible accelerograms. In this respect, future modifications of the Chinese aseismic code may prescribe a pseudo-acceleration design spectrum whose definition will extent to periods greater than 6s that will yield relative displacement design spectra converging to a constant spectral displacement for longer periods(see e.g. CEN, 2004). Ideally, this constant value should be set equal to a prescribed peak ground displacement, since it is well-established that the peak relative displacement response of very flexible linear SDOF systems subject to a strong ground motion coincides with the maximum displacement of the ground.

**6 Concluding remarks**

A numerical approach has been extended and customized to produce input acceleration time-histories for linear and nonlinear time-history analysis compatible with the pertinent criteria of the current Chinese aseismic code provisions (GB 50011-2001). The approach utilizes a stochastic dynamics formulation to generate artificial accelerograms and a harmonic wavelet based iterative procedure to modify signals individually to improve the matching of their response spectra with any given response/design spectrum. A flowchart of the adopted approach is shown in Fig. 10 to further elucidate the succession of the various involved steps and outcomes.

In the process of generating artificial accelerograms, a polynomial expression for the peak factor ratio as a function of natural period has been provided by fitting numerically derived data from appropriate Monte Carlo simulations associated with the GB 50011-2001 design spectrum. This expression has been incorporated in the derivation of GB 50011-2001 design spectrum

compatible evolutionary Kanai-Tajimi (K-T) spectra for all possible design spectra as defined by the Chinese aseismic code provisions. Furthermore, the aforementioned numerically derived analytic expression for the peak factor spectrum can be useful in performing structural reliability analyses for the design of new or for assessing the performance of existing structures in the context of the GB 50011-2001 regulations, since the peak factor is closely related to the first-passage problem of the random vibration theory (Vanmarcke, 1976).

Special attention has been also given to relating the shape of the time-envelop function used to modulate the K-T spectra with a commonly used definition of strong ground motion effective duration. In this manner, the stochastic dynamics formulation adopted herein can yield artificial seismic records of a pre-defined effective duration; an attribute which is critical when considering certain performance criteria within the framework of performance based design of structures (Iervolino et al., 2006; Hancock and Bommer, 2006).

Evolutionary K-T spectra compatible with all possible shapes and intensity levels of the GB 50011-2001 design spectrum have been provided in tabular form. These have been used to generate ensembles of artificial accelerograms whose average response spectra are in a close agreement with the GB 50011-2001 design spectrum. The level of this agreement is significantly enhanced compared to previous related research efforts using a constant peak factor (Spanos and Vargas Loli, 1985; Marano et al., 2008; Giaralis and Spanos, 2009), as opposed to the herein derived period dependent peak factor spectrum. Moreover, the reported K-T spectra can significantly facilitate the design process in applications necessitating accounting for the stochastic nature of the input strong ground motion in an explicit manner. Specifically, the K-T spectra corresponding to “minor” design earthquake level for which structures are required to behave elastically can be utilized in conjunction with linear random vibration formulations to obtain the probabilistic attributes of the response of multi DOF structures in preliminary stages of the structural design process. Similarly, the K-T spectra associated with the “major” design earthquake level can be considered as input to study the

stochastic features of the expected nonlinear/hysteretic response of multi DOF structures in the context of the statistical linearization method (Roberts and Spanos, 2003).

Furthermore, a specific design example necessitating time-history analysis to be performed has been considered to illustrate the efficiency of the considered harmonic wavelet iterative procedure to modify accelerograms to improve the agreement of their response spectrum with the GB design spectrum. In this context, small suites of accelerograms encompassing recorded time-histories associated with the magnitude 7.9 Wenchuan seismic event of May, 2008 and artificially generated signals compatible with a certain evolutionary K-T spectrum have been treated.

Finally, certain suggestions have been made for possible modification of the Chinese aseismic code of both the design spectrum and the compatibility criteria for the input accelerograms to be used for dynamic elastic and inelastic time-history analyses to incorporate, if desired, aspects of the aseismic design philosophy of other areas in the world.

**Appendix A. Design spectrum of the Chinese GB 50011-2001 aseismic code provisions**

The elastic pseudo-acceleration design spectrum for oscillators with 5% ratio of critical damping and natural period $T$, is defined by the current aseismic code provisions effective in China (GB 50011-2001) by the expression

$$S_a(T)=\begin{cases} a_{\max}\left(0.45+5.5T\right) & , \quad 0\le T\le 0.1 \\ a_{\max} & , \quad 0.1\le T\le T_g \\ a_{\max}\left(\dfrac{T_g}{T}\right)^{0.9} & , \quad T_g\le T\le 5T_g \\ a_{\max}\left[0.2^{0.9}-0.02\left(T-5T_g\right)\right] & , \quad 5T_g\le T\le 6 \end{cases}. \tag{A1}$$

In this equation, $\alpha_{max}$ is the peak value of the pseudo-acceleration spectral ordinate corresponding to the flat region of the design spectrum which ends at the characteristic (corner) period $T_g$, as depicted in the left plot of Fig. A1.

The value of $\alpha_{max}$ depends on a nominal peak ground acceleration associated with the local "intensity level" taken from the pertinent seismic hazard map of China and the returning period of the design earthquake considered as shown in table A1. In general, a two-phase performance based design procedure is mandated according to which structures should behave elastically under the "minor" or "frequent" earthquake of 50-years return period (63% probability of exceedance in a 50-years period of assumed life service), while they should not collapse under the "major" or "rare" design earthquake of 2000-years return period (2-3% probability of exceedance within 50-years) (see also Shiping (1993) and Wang (2004)).

The corner period $T_g$ can take on the values given in table A2 according to the "design seismic group" that the considered location of construction belongs to. The later is a function of the epicentral distance and the anticipated earthquake magnitude (e.g. Shiping, 1993). Further, the GB 50011-2001 code relates the corner period to the expected intensity level of the design earthquake by requiring to increase the values of $T_g$ of table A2 by 0.05sec for intensity levels 8 and 9. Thus, $T_g$ can overall attain 14 different values ranging from 0.25sec to 0.95sec (see also table 2).

The right panel of Fig. A1 plots the relative displacement design spectrum obtained from the pseudo-acceleration spectrum of Eq. (A1) via the equation

$$S_d(T) = \left(\frac{T}{2\pi}\right)^2 S_a(T). \qquad \text{(A2)}$$

The above $S_d$ spectrum is the one considered in section 5 to obtain compatible Kanai-Tajimi evolutionary power spectra for all possible combinations of $\alpha_{max}$ and $T_g$ defined in the GB 50011-2001 regulations.

**References**


Bogdanoff JL, Goldberg JE and Bernard MC (1961), "Response of a simple structure to a random earthquake-type disturbance," *Bulletin of the Seismological Society of America,* **51**(2): 293-310.

Bommer JJ and Martínez-Pereira A (1999), "The effective duration of earthquake strong motion," *Journal of Earthquake Engineering,* **3**(2): 127-172.

Bommer JJ and Ruggeri C (2002), "The specification of acceleration time-histories in seismic design codes," *European Earthquake Engineering,* **16**(1): 3-16.

Boore DM (2003), "Simulation of ground motion using the stochastic method," *Pure and Applied Geophysics,* **160**(3-4): 635-676.

Boore DM (2005), "On pads and filters: Processing strong-motion data," *Bulletin of the Seismological Society of America,* **95**(2): 745-750.

Boore DM and Akkar S (2003), "Effect of causal and acausal filters on elastic and inelastic response spectra," *Earthquake Engineering and Structural Dynamics,* **32**(11):1729-1748.

Boore DM and Bommer JJ (2005), "Processing of strong-motion accelerograms: needs, options and consequences," *Soil Dynamics and Earthquake Engineering,* **25**(2): 93-115.

Carballo JE and Cornell CA (2000), "Probabilistic seismic demand analysis: Spectrum matching and design," *Report RMS-41*, Department of Civil and Environmental Engineering, Stanford University.

CEN (2004), *Eurocode 8: Design of Structures for Earthquake Resistance – Part 1: General Rules, Seismic Actions and Rules for Buildings (EN 1998-1: 2004)*, Comité Européen de Normalisation, Brussels.

Chopra AK (2007), "Elastic response spectrum: A historical note," *Earthquake Engineering and Structural Dynamics,* **36**(1): 3-12.

Chopra AK and Lopez OA (1979), "Evaluation of simulated ground motions for predicting elastic response of long period structures and inelastic response of structures," *Earthquake Engineering and Structural Dynamics,* **7**(4): 383-402.

Clough RW and Penzien J (1993), *Dynamics of Structures*. *Second Edition*, Mc-Graw Hill, New York.

Conte JP, Pister KS and Mahin SA (1992), "Nonstationary ARMA modeling of seismic motions," *Soil Dynamics and Earthquake Engineering,* **11**(7): 411-426.

Converse AM and Brady AG (1992), "BAP: basic strong-motion accelerogram processing software, version 1.0," *Open File Report 92-296A*, United States Department of the interior Geological Survey.

Crespi PG, Floris C and Paganini P (2002), "A probabilistic method for generating spectrum compatible earthquake time histories," *European Earthquake Engineering,* **16**(3): 3-17.

Das S and Gupta VK (2008), "Wavelet-based simulation of spectrum-compatible aftershock accelerograms," *Earthquake Engineering and Structural Dynamics,* **37**(11): 1333-1348.

Faccioli E, Paolucci R and Rey J (2004), "Displacement spectra for long periods," *Earthquake Spectra*, **20**(2): 347-376.

Falsone G and Neri F (2000), "Stochastic modeling of earthquake excitation following the EC8: power spectrum and filtering equations," *European Earthquake Engineering,* **14**(1): 3-12.

GB 50011-2001 (2001), *Code for seismic design of buildings*, National Standard of the People's Republic of China, China Building Industry Press, Beijing.

Giaralis A and Spanos PD (2009), "Wavelet-based Response Spectrum Compatible Synthesis of Accelerograms- Eurocode Application (EC8)," *Soil Dynamics and Earthquake Engineering,* **29**(1): 219-235.

Gupta ID and Joshi RG (1993), "On synthesizing response spectrum compatible accelerograms," *European Earthquake Engineering,* **7**(2): 25-33.

Hancock J and Bommer JJ (2006), "A state-of-knowledge review of the influence of strong-motion duration on structural damage," *Earthquake Spectra*, **22**(3): 827-845.

Hancock J, Watson-Lamprey J, Abrahamson NA, Bommer JJ, Markatis A, McCoy E and Mendis R (2006), "An improved method of matching response spectra of recorded earthquake ground motion using wavelets," *Journal of Earthquake Engineering* **10**(1): 67-89.

ICC (2006), *International Building Code*, International Code Council, USA.

Iervolino I, Manfredi G and Cosenza E (2006), "Ground motion duration effects on nonlinear seismic response," *Earthquake Engineering and Structural Dynamics,* **35**(1): 21-38.

Iyama J and Kuwamura H (1999), "Application of wavelets to analysis and simulation of earthquake motions," *Earthquake Engineering and Structural Dynamics,* **28**(3): 255-272.

Jangid RS (2004), "Response of SDOF system to non-stationary earthquake excitation," *Earthquake Engineering and Structural Dynamics,* **33**(15): 1417-1428.

Kanai K (1957), "Semi-empirical formula for the seismic characteristics of the ground. University of Tokyo," *Bulletin of Earthquake Research Institute, University of Tokyo,* **35**: 309-325.

Karabalis DL, Cokkinides GJ, Rizos DC and Mulliken JS (2000), "Simulation of earthquake ground motions by a deterministic approach," *Advances in Engineering Software*, **31**(5): 329-338.

Kottke A and Rathje E (2008), "A semi-automated procedure fr selecting and scaling recorded earthquake motions for dynamic analysis," *Earthquake Spectra*, **24**(4): 911-932.

Kozin F (1989), "Autoregressive moving average models of earthquake records," *Probabilistic Engineering Mechanics,* **3**(2): 58-63.

Lai SP (1982), "Statistical characterization of strong ground motions using power spectral density function," *Bulletin of the Seismological Society of America,* **72**(1): 259-274.

Lam N, Wilson J and Hutchinson G (2000), "Generation of synthetic earthquake accelerograms using seismological modeling: A review," *Journal of Earthquake Engineering,* **4**(3): 321-354.

Lin C-CJ and Ghaboussi J (2001), "Generating multiple spectrum compatible accelerograms using stochastic neural networks," *Earthquake Engineering and Structural Dynamics,* **30**(7): 1021-1042.

Lutes LD and Lilhanand (1979), "Frequency content in earthquake simulation," *Journal of the Engineering Mechanics Division, ASCE,* **105**(EM1): 143-158.

Marano GC, Trentadue F, Morrone E and Amara L (2008), "Sensitivity Analysis of Optimum Stochastic Nonstationary Response Spectra under Uncertain Soil Parameters," *Soil Dynamics and Earthquake Engineering,* **28**(12): 1078-1093.

Mason AB and Iwan WD (1983), "An approach to the first passage problem in random vibration," *Journal of Applied Mechanics, ASME,* **50**(): 641-646.

Michaelov G, Lutes LD and Sarkani S (2001), "Extreme value of response to nonstationary excitation," *Journal of Engineering Mechanics,* **127**(4): 352-363.

Morikawa H and Zerva A (2008), "Approximate representation of the statistics for extreme responses of single degree-of-freedom system excited by non-stationary processes," *Probabilistic Engineering Mechanics*, **23**(3): 279-288.

Mukherjee S and Gupta VK (2002), "Wavelet-based generation of spectrum-compatible time-histories," *Soil Dynamics and Earthquake Engineering,* **22**(9-12): 799-804.

Naeim F, Alimoradi A and Pezeshk S (2004), "Selection and scaling of ground motion time histories for structural design using genetic algorithms," *Earthquake Spectra* **20**(2): 413-426.

Newland DE (1994), "Harmonic and musical wavelets," *Proceedings of the Royal Society of London. Series A,* **444**(1921): 605-620.

Newland DE (1998), "Time-frequency and time-scale signal analysis by harmonic wavelets," in A. Procházka, J. Uhlír, P.J.W. Rayner and N.G. Kingsbury, editors, *Signal analysis and prediction*, Chapter 1, Birkhaüser, Boston.

Nocedal J and Wright SJ (1999), *Numerical Optimization*, Springer- Verlag, New York.

Ólafsson S, Remseth S and Sigbjornsson R (2001), "Stochastic models for simulation of strong ground motion in Iceland," *Earthquake Engineering and Structural Dynamics*, **30**(9): 1305-1331.

Politis NP, Giaralis A and Spanos PD (2007), "Joint time-frequency representation of simulated earthquake accelerograms via the adaptive chirplet transform," in G. Deodatis and P.D. Spanos, editors, *Computational Stochastic Mechanics-5*, Millpress, Rotterdam.

Preumont A (1984), "The generation of spectrum compatible accelerograms for the design of nuclear power plants," *Earthquake Engineering and Structural Dynamics*, **12**(4): 481-497.

Priestley MB (1965), "Evolutionary spectra and non-stationary processes," *Journal of the Royal Statistical Society. Series B,* **27**(2): 204-237.

Quek S-T, Teo Y-P and Balendra T (1990), "Non-stationary structural response with evolutionary spectra using seismological input model," *Earthquake Engineering and Structural Dynamics*, **19**(2): 275-288.

Roberts JB and Spanos PD (2003), *Random Vibration and Statistical Linearization*, Dover Publications, New York.

Shiping Hu (1993), "Seismic design of buildings in China," *Earthquake Spectra*, **9**(4): 703-737.

Shrikhande M and Gupta VK (1996), "On generating ensemble of design spectrum-compatible accelerograms," *European Earthquake Engineering,* **10**(3): 49-56.

Spanos PD (1983), "Digital synthesis of response-design spectrum compatible earthquake records for dynamic analyses," *The Shock and Vibration Digest*, **15**(3): 21-30.

Spanos PD and Lutes LD (1980), "Probability of response to evolutionary process," *Journal of the Engineering Mechanics Division, ASCE,* **106**(EM2): 213-224.

Spanos PD and Vargas Loli LM (1985), "A statistical approach to generation of design spectrum compatible earthquake time histories," *Soil Dynamics and Earthquake Engineering,* **4**(1): 2-8.

Spanos PD and Zeldin BA (1998), "Monte Carlo treatment of random fields: A broad perspective," *Applied Mechanics Reviews* **51**(3): 219-237.

Spanos PD, Tezcan J and Tratskas P (2005), "Stochastic processes evolutionary spectrum estimation via harmonic wavelets," *Computer Methods in Applied Mechanics and Engineering,* **194**(12-16): 1367-1383.

Spanos PD, Giaralis A, Politis NP and Roesset JM (2007), "Numerical treatment of seismic accelerograms and of inelastic seismic structural responses using harmonic wavelets," *Computer-Aided Civil and Infrastructure Engineering,* **22**(4): 254-264.

Suárez LE and Montejo LA (2005), "Generation of artificial earthquakes via the wavelet transform," *International Journal of Solids and Structures,* **42**(21-22): 5905-5919.

Suárez LE and Montejo LA (2007), "Application of the wavelet transform in the generation and analysis of spectrum-compatible records," *Structural Engineering and Mechanics,* **27**(2): 173-197.

Trifunac MD and Brady AG (1975), "A study on the duration of strong earthquake ground motion," *Bulletin of the Seismological Society of America*, **65**(3): 581-626.

Vanmarcke EH (1976), "Structural response to earthquakes," in C. Lomnitz and E. Rosenblueth, editors, Seismic Risk and Engineering Decisions, Chapter 8, Elsevier, Amsterdam.

Wang Yayong (2004), "Comaprison of seismic actions and structural design requirements in Chinese Code GB 50011 and International Standard ISO 3010," *Earthquake Engineering and Engineering Vibrations* **3**(1): 1-9.

Wang Junjie, Fan Lichu, Qian Shie and Zhou Jing (2002), "Simulations of non-stationary frequency content and its importance to seismic assessment of structures," *Earthquake Engineering and Structural Dynamics*, **31**(4): 993-1005.

Wen YK and Gu Ping (2004), "Description and simulation of nonstationary processes based on Hilbert spectra," Journal of Engineering Mechanics, ASCE, **130**(8): 942-951.

| | | | |
|---|---|---|---|
| $p_0$: 3.0672 | $p_1$: -3.1765 | $p_2$: 3.7134 | $p_3$: -2.3920 |
| $p_4$: 0.8660 | $p_5$: -0.1760 | $p_6$: 0.0187 | $p_7$: -0.0008 |

**Table 1:** Polynomial coefficients of the fitted average peak factor spectrum of Eq. (28).

| **Design earthquake level** (return period) | **Level of intensity** (Peak ground acceleration) **6** (0.05g) | **7** (0.10g/ 0.15g) | **8** (0.20g/ 0.30g) | **9** (0.40g) |
|---|---|---|---|---|
| **Frequent earthquake** (50 years) | 0.04g | 0.08g/ 0.12g | 0.16g/ 0.24g | 0.36g |
| **Rare earthquake** (2000 years) | - | 0.50g/ 0.72g | 0.90g/ 1.20g | 1.40g |

**Table A1** Maximum value of the pseudo-acceleration spectral ordinate $\alpha_{max}$ (GB 50011-2001)

| **Design Earthquake group** | **Soil type** **1** | **2** | **3** | **4** |
|---|---|---|---|---|
| **1st group** | 0.25 | 0.35 | 0.45 | 0.65 |
| **2nd group** | 0.3 | 0.4 | 0.55 | 0.75 |
| **3rd group** | 0.35 | 0.45 | 0.65 | 0.9 |

**Table A2** Characteristic (corner) period $T_g$ (GB 50011-2001)

| $T_g$ (s) | $\alpha_{amax}$ (g) | $C$ (cm/s$^{2.5}$) | $b$ (s$^{-1}$) | $\xi_g$ | $\omega_g$ (rad/s) |
|---|---|---|---|---|---|
| **0.25** | **0.04** | 0.28 | 0.46 | 0.69 | 34.26 |
| | **0.08** | 0.57 | 0.48 | 0.73 | 31.60 |
| | **0.12** | 0.88 | 0.49 | 0.74 | 30.56 |
| | **0.16** | 1.18 | 0.49 | 0.75 | 30.10 |
| | **0.24** | 1.78 | 0.50 | 0.75 | 29.82 |
| | **0.32** | 2.37 | 0.49 | 0.75 | 29.81 |
| | **0.50** | 3.68 | 0.49 | 0.75 | 29.91 |
| | **0.72** | 5.71 | 0.53 | 0.75 | 29.68 |
| **0.30** | **0.04** | 0.27 | 0.40 | 0.68 | 25.96 |
| | **0.08** | 0.55 | 0.41 | 0.71 | 24.29 |
| | **0.12** | 0.84 | 0.42 | 0.72 | 23.86 |
| | **0.16** | 1.12 | 0.42 | 0.72 | 23.94 |
| | **0.24** | 1.71 | 0.42 | 0.73 | 24.30 |
| | **0.32** | 2.24 | 0.42 | 0.73 | 24.38 |
| | **0.50** | 3.29 | 0.39 | 0.72 | 24.36 |
| | **0.72** | 6.52 | 0.54 | 0.70 | 23.87 |
| | **0.90** | 8.76 | 0.58 | 0.69 | 23.84 |
| | **1.20** | 12.12 | 0.60 | 0.69 | 23.66 |
| | **1.40** | 12.67 | 0.54 | 0.70 | 23.82 |
| **0.35** | **0.04** | 0.26 | 0.35 | 0.67 | 21.56 |
| | **0.08** | 0.54 | 0.36 | 0.69 | 20.42 |
| | **0.12** | 0.82 | 0.37 | 0.70 | 20.32 |
| | **0.16** | 1.11 | 0.37 | 0.71 | 20.58 |
| | **0.24** | 1.67 | 0.37 | 0.71 | 20.74 |
| | **0.32** | 2.16 | 0.36 | 0.71 | 20.74 |
| | **0.50** | 4.23 | 0.46 | 0.69 | 20.36 |
| | **0.72** | 6.91 | 0.52 | 0.67 | 20.27 |
| | **0.90** | 9.52 | 0.57 | 0.66 | 19.98 |
| | **1.20** | 12.63 | 0.57 | 0.65 | 19.70 |
| | **1.40** | 14.13 | 0.55 | 0.65 | 19.62 |
| **0.40** | **0.04** | 0.26 | 0.32 | 0.66 | 18.52 |
| | **0.08** | 0.53 | 0.33 | 0.67 | 17.78 |
| | **0.12** | 0.80 | 0.33 | 0.68 | 17.84 |
| | **0.16** | 1.08 | 0.33 | 0.69 | 18.01 |
| | **0.24** | 1.59 | 0.33 | 0.69 | 18.09 |
| | **0.32** | 2.07 | 0.32 | 0.68 | 18.07 |
| | **0.50** | 4.38 | 0.44 | 0.64 | 17.81 |
| | **0.72** | 7.50 | 0.52 | 0.64 | 17.38 |
| | **0.90** | 10.37 | 0.57 | 0.62 | 16.97 |
| | **1.20** | 15.55 | 0.65 | 0.72 | 15.67 |
| | **1.40** | 23.94 | 0.73 | 0.79 | 13.83 |
| **0.45** | **0.04** | 0.25 | 0.29 | 0.64 | 16.08 |
| | **0.08** | 0.51 | 0.29 | 0.65 | 15.73 |
| | **0.12** | 0.78 | 0.30 | 0.66 | 15.97 |
| | **0.16** | 1.04 | 0.30 | 0.67 | 16.06 |
| | **0.24** | 1.52 | 0.29 | 0.66 | 16.07 |
| | **0.32** | 2.50 | 0.36 | 0.65 | 15.83 |
| | **0.50** | 4.68 | 0.43 | 0.63 | 15.65 |
| | **0.72** | 7.96 | 0.51 | 0.60 | 15.12 |
| | **0.90** | 14.65 | 0.64 | 0.78 | 12.45 |
| | **1.20** | 20.11 | 0.65 | 0.79 | 12.22 |
| | **1.40** | 22.13 | 0.63 | 0.78 | 12.50 |
| **0.50** | **0.90** | 14.63 | 0.59 | 0.79 | 11.05 |
| | **1.20** | 20.14 | 0.60 | 0.80 | 10.86 |
| | **1.40** | 21.73 | 0.57 | 0.79 | 11.12 |
| **0.55** | **0.04** | 0.22 | 0.23 | 0.61 | 12.75 |
| | **0.08** | 0.47 | 0.24 | 0.63 | 13.16 |
| | **0.12** | 0.71 | 0.24 | 0.63 | 13.24 |
| | **0.16** | 0.92 | 0.23 | 0.63 | 13.24 |
| | **0.24** | 1.89 | 0.32 | 0.60 | 12.96 |
| | **0.32** | 2.78 | 0.36 | 0.58 | 12.84 |
| | **0.50** | 5.21 | 0.43 | 0.58 | 12.43 |
| | **0.72** | 11.64 | 0.55 | 0.78 | 10.14 |
| **0.60** | **0.90** | 14.62 | 0.51 | 0.81 | 9.11 |
| | **1.20** | 19.20 | 0.51 | 0.81 | 9.06 |
| | **1.40** | 19.87 | 0.45 | 0.80 | 9.21 |
| **0.65** | **0.04** | 0.21 | 0.20 | 0.61 | 11.31 |
| | **0.08** | 0.42 | 0.19 | 0.61 | 11.37 |
| | **0.12** | 0.59 | 0.18 | 0.60 | 11.37 |
| | **0.16** | 1.14 | 0.26 | 0.59 | 11.13 |
| | **0.24** | 2.02 | 0.31 | 0.57 | 10.95 |
| | **0.32** | 4.98 | 0.48 | 0.76 | 8.90 |
| | **0.50** | 7.55 | 0.46 | 0.78 | 8.66 |
| | **0.72** | 11.29 | 0.47 | 0.80 | 8.50 |
| **0.70** | **0.90** | 14.55 | 0.46 | 0.84 | 7.72 |
| | **1.20** | 20.54 | 0.48 | 0.86 | 7.59 |
| | **1.40** | 24.81 | 0.49 | 0.88 | 7.52 |
| **0.75** | **0.04** | 0.21 | 0.18 | 0.61 | 10.21 |
| | **0.08** | 0.41 | 0.17 | 0.60 | 10.09 |
| | **0.12** | 0.83 | 0.23 | 0.59 | 9.84 |
| | **0.16** | 1.25 | 0.26 | 0.58 | 9.71 |
| | **0.24** | 2.23 | 0.31 | 0.56 | 9.30 |
| | **0.32** | 4.55 | 0.40 | 0.78 | 7.60 |
| | **0.50** | 7.37 | 0.41 | 0.80 | 7.44 |
| | **0.72** | 11.22 | 0.42 | 0.83 | 7.27 |
| **0.80** | **0.90** | 14.87 | 0.42 | 0.86 | 6.64 |
| | **1.20** | 21.18 | 0.45 | 0.89 | 6.53 |
| | **1.40** | 25.36 | 0.45 | 0.90 | 6.49 |
| **0.90** | **0.04** | 0.22 | 0.16 | 0.63 | 8.82 |
| | **0.08** | 0.99 | 0.31 | 0.94 | 7.22 |
| | **0.12** | 1.63 | 0.33 | 0.84 | 6.40 |
| | **0.16** | 2.22 | 0.34 | 0.81 | 6.26 |
| | **0.24** | 3.38 | 0.34 | 0.81 | 6.18 |
| | **0.32** | 4.59 | 0.35 | 0.82 | 6.12 |
| | **0.50** | 7.58 | 0.36 | 0.85 | 5.99 |
| | **0.72** | 11.87 | 0.39 | 0.88 | 5.84 |
| **0.95** | **0.90** | 16.48 | 0.41 | 0.93 | 5.40 |
| | **1.20** | 22.23 | 0.41 | 0.94 | 5.38 |
| | **1.40** | 25.89 | 0.41 | 0.95 | 5.38 |
| | **0.50** | 14.63 | 0.59 | 0.79 | 11.05 |
| | **0.72** | 20.14 | 0.60 | 0.80 | 10.86 |

**Table 2:** Parameters for the definition of K-T evolutionary power spectra compatible with the GB 50011-2001 design spectrum for all possible combinations of $T_g$ and $\alpha_{max}$ parameters (see also Appendix A).

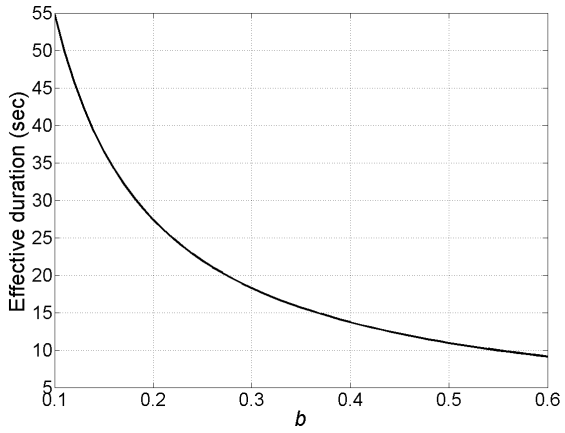


**Fig. 1** Relationship between the effective duration, as defined in Trifunac and Brady (1975), and the shape parameter $b$ in Eq. (3).

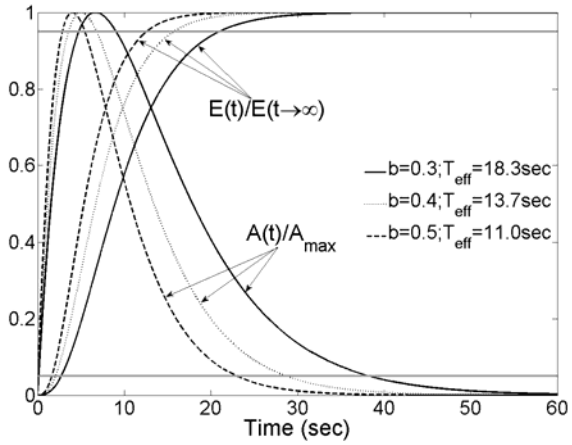


**Fig. 2** Plots of the envelop function of Eq. (3) and cumulative energy of Eq. (4) normalized to their peak values for different shape parameters $b$. The lower and upper horizontal lines correspond to 5% and 95% of total energy, respectively, signifying the beginning and the end of the strong ground motion effective duration (Trifunac and Brady, 1975).

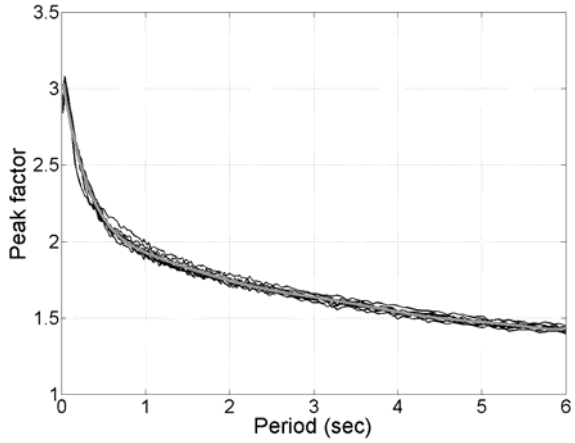


**Fig. 3** Peak factor spectra obtained by Eq. (27) pertaining to the GB 50011-2001 design spectrum for all 14 different values of $T_g$ (thin black lines) and average peak factor spectrum given by Eq. (28) (thick gray line).

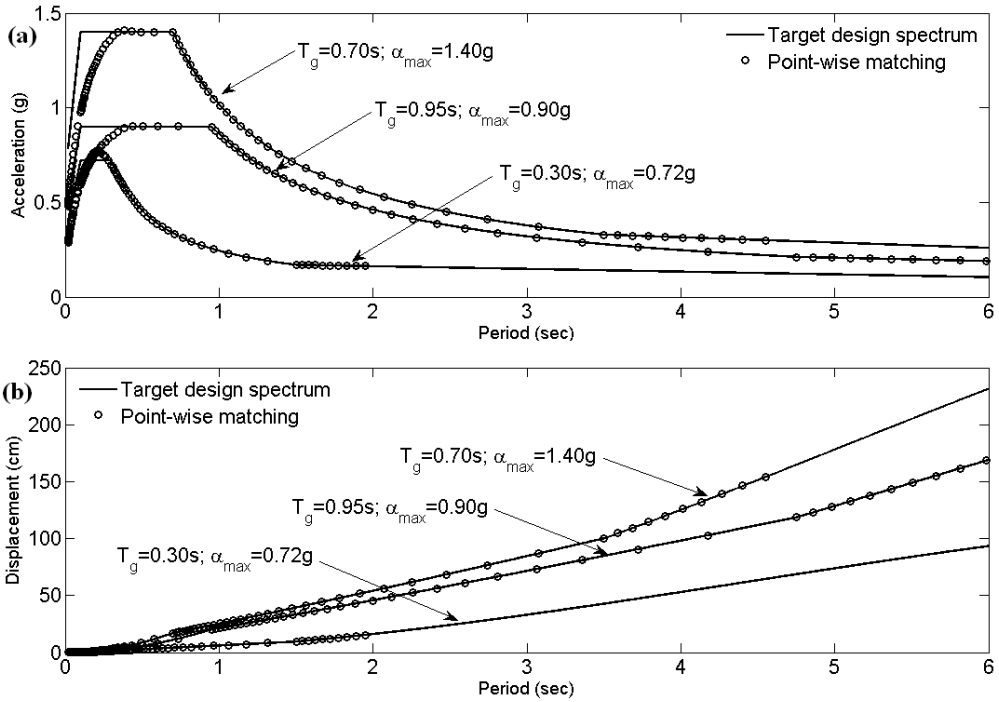


**Fig. 4** Point-wise least-square matching for specific K-T evolutionary spectra included in Table 2 in terms of pseudo-acceleration (a) and relative displacement (b) spectral ordinates.

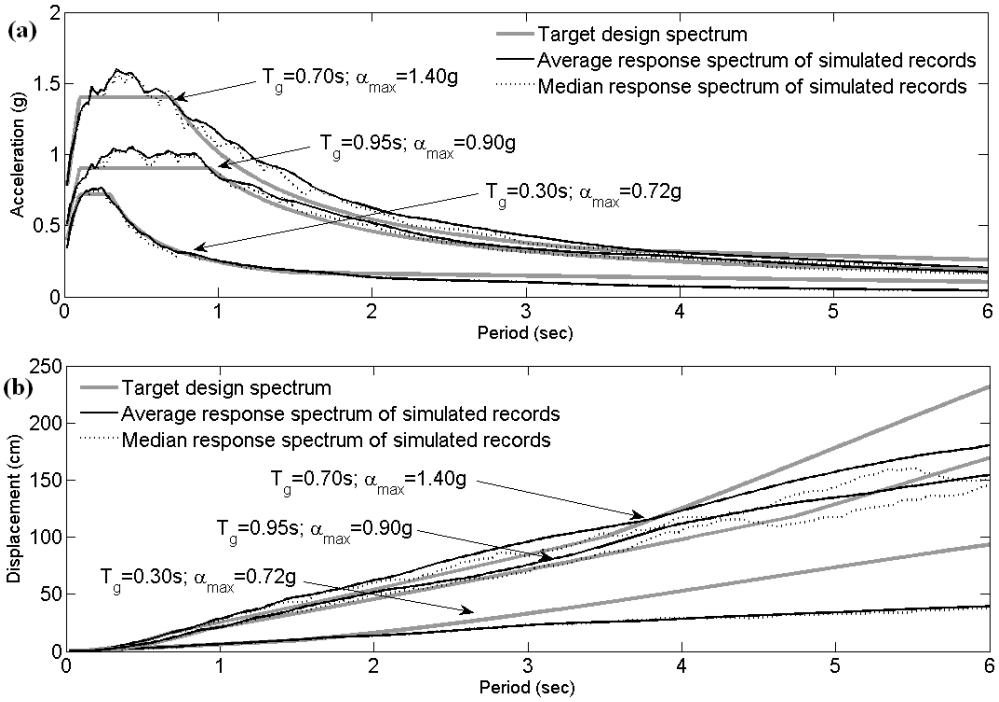


**Fig. 5** Pseudo-acceleration (a) and relative displacement (b) response spectra of ensembles of simulated and baseline corrected accelerograms compatible with the K-T evolutionary spectra corresponding to various GB 50011-2001 design spectra. Each ensemble considered includes 40 signals.

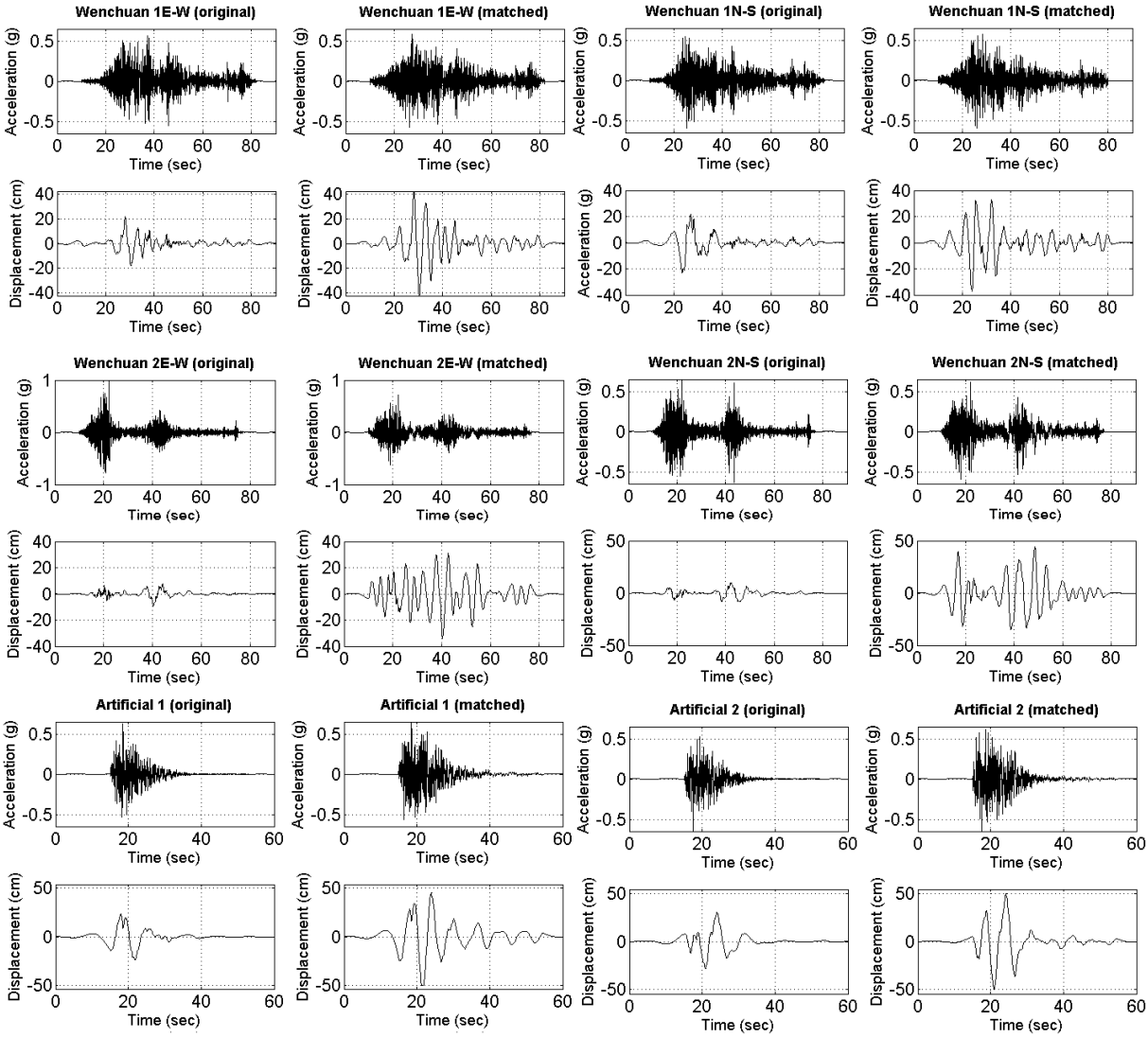


**Fig. 6** Base line corrected acceleration and displacement traces of all recorded and artificial signals considered in the design example before and after processing via the iterative modification procedure to match the GB 50011-2001 design spectrum for $T_g$= 0.40s and $\alpha_{max}$= 1.40g. Eight iterations have been performed with harmonic wavelet basis of uniform scale bandwidths: $n$-$m$= 6 and $\Delta\omega$= 0.0767rad/s.

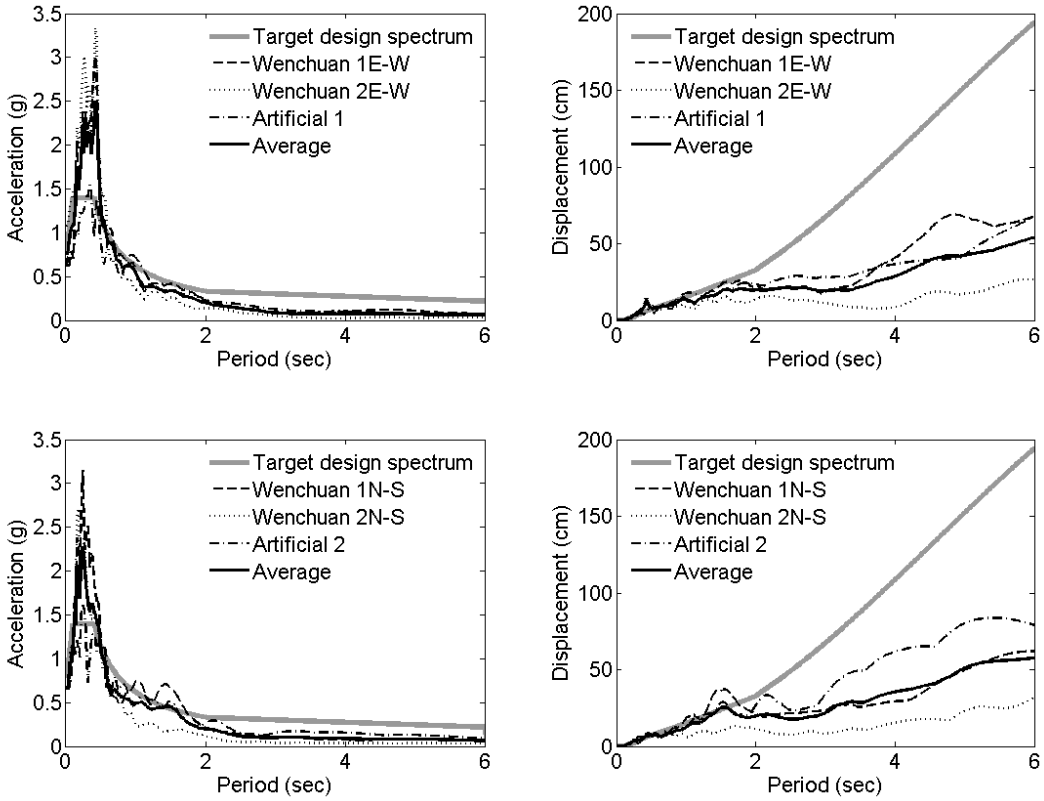


Fig. 7 Individual and average pseudo-acceleration and relative displacement response spectra of the original signals shown in Fig. 6.

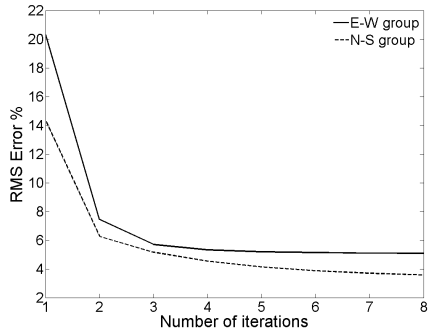


Fig. 8 Quality of matching of average response spectra with the target spectrum in terms of the RMS error (Eq. (29)) as a function of the number of iterations performed.

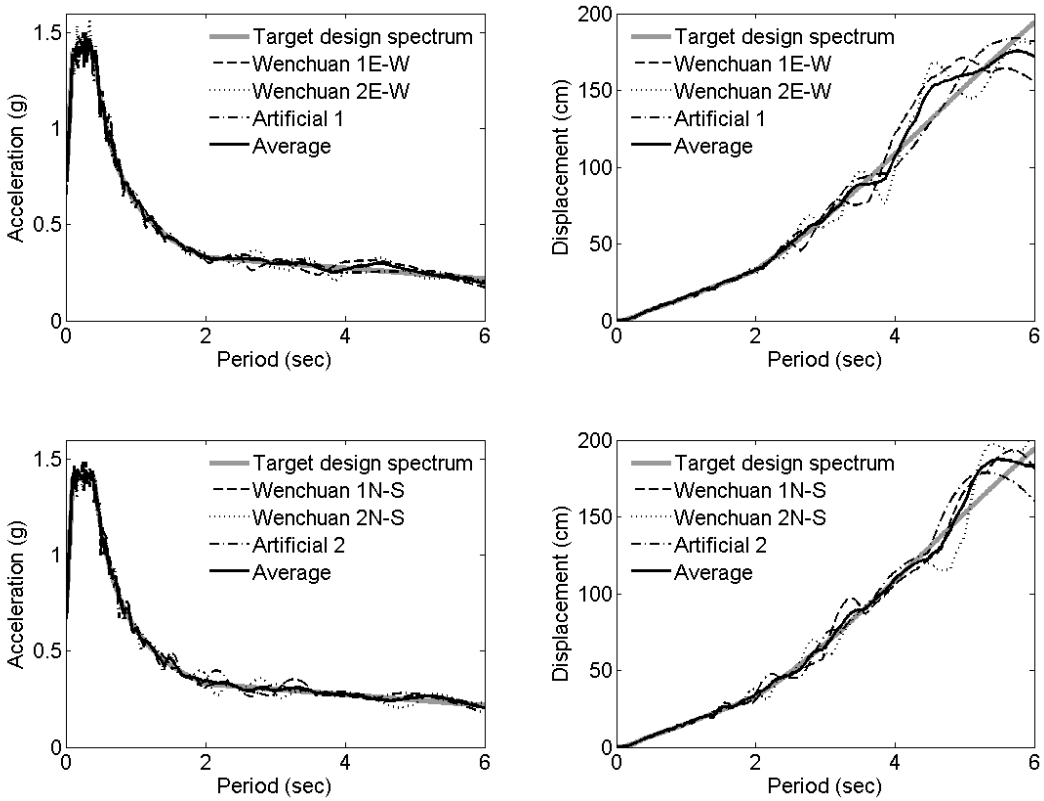


Fig. 9 Individual and average pseudo-acceleration and relative displacement response spectra of the modified signals shown in Fig. 6.

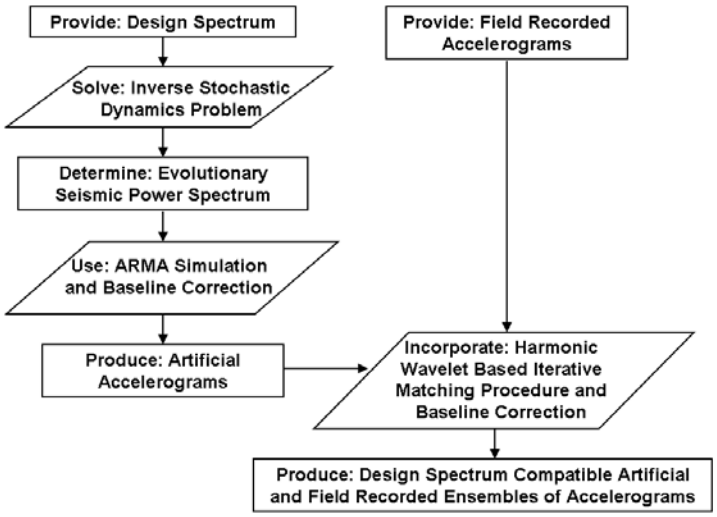


Fig. 10 Flowchart of the adopted approach.

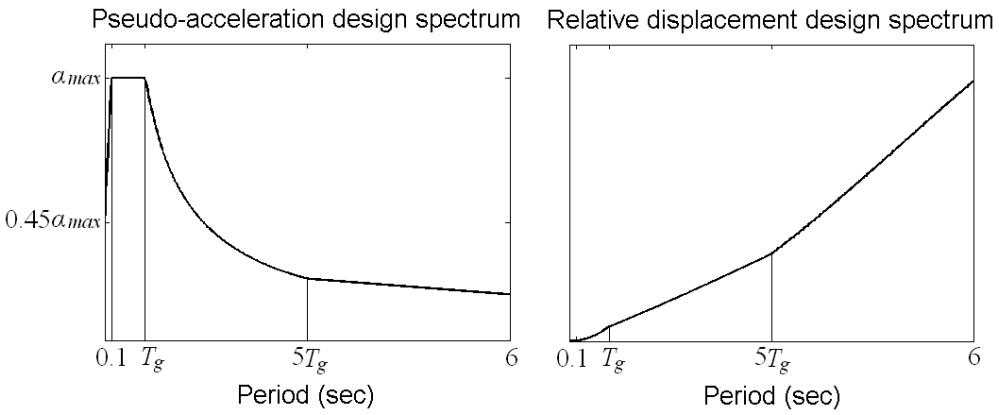


**Fig. A1** Graphical representation of the elastic pseudo-acceleration (Eq. (A1)) and relative displacement (Eq. (A2)) design spectra of the GB 50011-2001.